

## NONLINEAR BAROCLINIC HAURWITZ WAVES

Zhang Xuehong (张学洪), Zeng Qingcun (曾庆存) and Bao Ning (包宁)

Institute of Atmospheric Physics, Academia Sinica, Beijing

Received July 30, 1985

### ABSTRACT

A family of nonlinear wave solutions, with Haurwitz waves as their zero-order approximations, to the baroclinic primitive equations is derived and the corresponding calculating system is presented. Numerical experiments with a two-level global model developed by ourselves confirm the validity of the theoretical results to a great extent.

### I. INTRODUCTION

Haurwitz waves are a family of special solutions to the barotropic vorticity equation on sphere<sup>[1]</sup>. They have been widely used in the testing of numerical weather prediction models and general circulation ones since Phillips' paper<sup>[2]</sup> published. Using a perturbation method, Zeng Qingcun<sup>[3]</sup> has obtained nonlinear versions of certain Haurwitz waves.

Our recent investigation<sup>[4]</sup> has shown that certain Haurwitz waves with weak baroclinicity can be regarded as the zero-order approximations of some travelling wave solutions to the baroclinic primitive equations on sphere. In this paper, we shall derive the governing equations of nonlinear Haurwitz waves, construct a calculating system for nonlinear Haurwitz waves in a two-level model and describe some preliminary results from numerical experiments.

### II. PERTURBATION EQUATIONS

Introducing stream function  $\Psi$  and velocity potential  $\chi$ , we are able to write the baroclinic primitive equations on sphere as follows:

$$\left\{ \begin{aligned} & \frac{\partial}{\partial t} \Delta \Psi + J(\Psi, \Omega_0) + \nabla \chi \cdot \nabla \Omega_0 + \sigma \frac{\partial}{\partial \sigma} \Delta \Psi + \nabla \left( \frac{\partial \Psi}{\partial \sigma} \right) \cdot \nabla \sigma - J \left( \frac{\partial \chi}{\partial \sigma}, \sigma \right) \\ & = -\Omega_0 \Delta \chi - \frac{R}{p_{**}} J(T', p'_{**}), \\ & \frac{\partial}{\partial t} \Delta \chi + J(\chi, \Omega_0) - \nabla \Psi \cdot \nabla \Omega_0 + \sigma \frac{\partial}{\partial \sigma} \Delta \chi + J \left( \frac{\partial \Psi}{\partial \sigma}, \sigma \right) + \nabla \left( \frac{\partial \chi}{\partial \sigma} \right) \cdot \nabla \sigma \\ & = \Omega_0 \Delta \Psi - \Delta \Phi - \frac{RT'}{p_{**}} \Delta p'_{**} - R \nabla \left( \frac{T'}{p_{**}} \right) \cdot \nabla p'_{**}, \\ & \frac{\partial T'}{\partial t} + J(\Psi, T') + \nabla \chi \cdot \nabla T' + \sigma \frac{\partial T'}{\partial \sigma} \end{aligned} \right. \quad (1)$$

$$\begin{aligned}
 &= \left[ \frac{\bar{c}_0^2}{R} \frac{S^2}{\sigma} + \left( \frac{p_t}{p_{cs}} \frac{S}{\sigma^2} + \delta \kappa \frac{S}{\sigma} \right) T' \right] \left( \dot{\sigma} + \frac{\sigma}{p_{cs}} \frac{dp'_{cs}}{dt} \right) \\
 \left. \begin{aligned}
 \frac{dp'_{cs}}{dt} &\equiv \frac{\partial p'_{cs}}{\partial t} + J(\Psi, p'_{cs}) + \nabla \chi \cdot \nabla p'_{cs} = -p_{cs} \left( \Delta \chi + \frac{\partial \dot{\sigma}}{\partial \sigma} \right), \\
 T' &= -\frac{\sigma}{R} \frac{\partial \phi'}{\partial \sigma}, \\
 \Omega_s &\equiv 2\omega \cos \theta + \Delta \Psi, \quad \Phi \equiv \phi' + \frac{1}{2} [ |\nabla \Psi|^2 + |\nabla \chi|^2 + 2J(\Psi, \chi) ]
 \end{aligned} \right\}
 \end{aligned}$$

where  $\sigma$  is a normalized pressure coordinate and  $J$ ,  $\nabla$  and  $\Delta$  are Jacobian, gradient and Laplacian operators, respectively.

With characteristic horizontal scale  $L^*$ , characteristic time scale  $t^*$ , characteristic wind velocity  $U^*$ , characteristic surface pressure disturbance  $P^*$ , characteristic horizontal geopotential disturbance  $\Phi^*$  and characteristic vertical geopotential disturbance  $\Phi^{**}$  given, the following dimensionless parameters can be defined:

$$\left\{ \begin{aligned}
 \bar{\mu}^{-1} &\equiv \frac{L^*}{a}, & \varepsilon &\equiv \frac{1}{2\omega t^*}, & \varepsilon' &\equiv \frac{U^*}{2\omega L^*}, \\
 \varepsilon'' &\equiv \frac{P^*}{p_{cs}}, & \varepsilon''' &\equiv \frac{\Phi^*}{\bar{c}_0^2}, & \varepsilon^* &\equiv \frac{\Phi^{**}}{\Phi^*},
 \end{aligned} \right. \quad (2)$$

where  $a$  is the radius of the earth,  $\omega$  the angular velocity of earth's rotation,  $p_{cs}$  the equivalent average surface pressure and  $\bar{c}_0$  the speed of the inertio-gravitational wave under a certain standard atmosphere. For slow processes of the flow with large scale and low velocity, we can take  $\varepsilon' = \varepsilon \ll 1$ ,  $\bar{\mu}^{-1} = \delta_\mu \varepsilon$  and  $\varepsilon''' = \delta''' \varepsilon$ . Furthermore, under the assumptions of weak baroclinicity and weak compressibility, we have  $\varepsilon^* = \delta^* \varepsilon$  and  $\varepsilon'' = \delta'' \varepsilon^2$ . Here,  $\delta_\mu, \delta'''$ ,  $\delta^*$  and  $\delta''$  are the constants with the magnitude of order  $O(1)$ . Thus, the dimensionless form of (1) can be written as follows:

$$\left\{ \begin{aligned}
 \varepsilon \left[ -\frac{\partial}{\partial t} \hat{\Delta} \Psi + J(\Psi, \hat{\Delta} \Psi) + \delta_\mu \frac{\partial}{\partial \lambda} \Psi \right] &= -\cos \theta \hat{\Delta} \chi + \varepsilon \cdot O(\chi, \dot{\sigma}, \varepsilon^2), \\
 \hat{\Delta} \phi' &= \cos \theta \hat{\Delta} \Psi - \varepsilon N(\Psi) + \varepsilon \cdot O(\chi, \dot{\sigma}, \varepsilon^2), \\
 \left( \frac{S^2}{\sigma} \right) \dot{\sigma} &= \delta''' \delta^* \varepsilon^2 \left[ \frac{\partial T'}{\partial t} + J(\Psi, T') \right] + \varepsilon^2 \cdot O(\chi, \dot{\sigma}, \varepsilon^2), \\
 \hat{\Delta} \chi + \frac{\partial \dot{\sigma}}{\partial \sigma} &= -\varepsilon^2 \delta'' \left[ \frac{\partial p'_{cs}}{\partial t} + J(\Psi, p'_{cs}) \right] + \varepsilon^2 \cdot O(\chi), \\
 T' &= -\frac{\sigma}{\varepsilon^*} \frac{\partial \phi'}{\partial \sigma},
 \end{aligned} \right. \quad (3)$$

where

$$\left\{ \begin{aligned}
 \frac{\hat{\partial}}{\partial \theta} &\equiv \bar{\mu}^{-1} \frac{\partial}{\partial \theta}, & \frac{\hat{\partial}}{\partial \lambda} &\equiv \bar{\mu}^{-1} \frac{\partial}{\partial \lambda}, \\
 J(F, G) &\equiv \frac{1}{\sin \theta} \left( \frac{\hat{\partial}}{\partial \theta} F \frac{\hat{\partial}}{\partial \lambda} G - \frac{\hat{\partial}}{\partial \theta} G \frac{\hat{\partial}}{\partial \lambda} F \right),
 \end{aligned} \right.$$

$$\hat{\nabla} F \cdot \hat{\nabla} G \equiv \frac{\hat{\partial}}{\partial \theta} F \frac{\hat{\partial}}{\partial \theta} G + \frac{1}{\sin^2 \theta} \frac{\hat{\partial}}{\partial \lambda} F \frac{\hat{\partial}}{\partial \lambda} G, \quad (4)$$

$$\hat{\Delta} \equiv \frac{1}{\sin \theta} \frac{\hat{\partial}}{\partial \theta} \left( \sin \theta \frac{\hat{\partial}}{\partial \theta} \right) + \frac{1}{\sin^2 \theta} \frac{\hat{\partial}}{\partial \lambda} \frac{\hat{\partial}}{\partial \lambda}$$

Expanding the variables and their governing equations (1) in the power series of the small parameter  $\epsilon$ , we obtain the following zero-order and first-order problems:

$$\begin{aligned} \chi_0 = \dot{\sigma}_0 = 0, \quad \chi_1 = \dot{\sigma}_1 = 0, \\ \frac{\partial}{\partial t} \hat{\Delta} \Psi_0 + J(\Psi_0, \hat{\Delta} \Psi_0) + \delta_\mu \frac{\hat{\partial}}{\partial \lambda} \Psi_0 = 0, \\ \hat{\Delta} \phi'_0 = \cos \theta \hat{\Delta} \Psi_0 - \epsilon N(\Psi_0), \\ T'_{00} = -\frac{\sigma}{\epsilon^*} \frac{\partial \phi'_0}{\partial \sigma}, \\ p'_{00} = \frac{p_0}{RT_0} \cdot \phi'_{00} \end{aligned} \quad (5)$$

and

$$\begin{aligned} \dot{\sigma}_2 = \delta''' \delta^* \left( \frac{\sigma}{S_2} \right) \left[ \frac{\partial T'_{00}}{\partial t} + J(\Psi_0, T'_{00}) \right], \\ \hat{\Delta} \chi_1 = -\frac{\partial \dot{\sigma}_2}{\partial \sigma} - \delta'' \left[ \frac{\partial p'_{00}}{\partial t} + J(\Psi_0, p'_{00}) \right] \\ \frac{\partial}{\partial t} \hat{\Delta} \Psi_1 + J(\Psi_0, \hat{\Delta} \Psi_1) + J(\Psi_1, \hat{\Delta} \Psi_0) + \delta_\mu \frac{\hat{\partial}}{\partial \lambda} \Psi_1 = -\cos \theta \hat{\Delta} \chi_1, \\ \hat{\Delta} \phi'_1 = \cos \theta \hat{\Delta} \Psi_1 - \epsilon N_1(\Psi_0, \Psi_1), \\ T'_{10} = -\frac{\sigma}{\epsilon^*} \frac{\partial \phi'_1}{\partial \sigma}, \\ p'_{10} = \frac{p_1}{RT_1} \cdot \phi'_{10} \end{aligned} \quad (6)$$

where

$$\begin{aligned} N(\Psi) &\equiv \delta_\mu \sin \theta \frac{\hat{\partial}}{\partial \theta} \Psi - (\hat{\Delta} \Psi)^2 - \hat{\nabla} \Psi \cdot \hat{\nabla} (\hat{\Delta} \Psi) + \frac{1}{2} \hat{\Delta} (|\hat{\nabla} \Psi|^2), \\ N_1(\Psi_0, \Psi_1) &\equiv \delta_\mu \sin \theta \frac{\hat{\partial}}{\partial \theta} \Psi_1 - 2 \hat{\Delta} \Psi_0 \hat{\Delta} \Psi_1 - \hat{\nabla} \Psi_0 \cdot \hat{\nabla} (\hat{\Delta} \Psi_1) - \hat{\nabla} \Psi_1 \cdot \hat{\nabla} (\hat{\Delta} \Psi_0) \\ &\quad + \hat{\Delta} (\hat{\nabla} \Psi_0 \cdot \hat{\nabla} \Psi_1). \end{aligned}$$

It should be pointed out that the Haurwitz wave given by Phillips is just a kind of formal solution to (5). Therefore, Eqs. (5) and (6) together constitute the governing equations of nonlinear Haurwitz waves.

### III. COMPUTER METHOD TO COMPLETE CERTAIN SPHERICAL HARMONIC OPERATIONS

With Haurwitz waves taken as the zero-order approximation (hereafter referred to as 0-Ax) of  $\Psi$ , we have to manage numerous nonlinear operations of spherical harmonics in

solving Eqs. (5) and (6). Instead of manual calculation, we tend to find a kind of computer method to complete the operations along the lines of Ref. [5]

Define a family of polynomials  $\{Q_l^k(x)\}$ , where

$$Q_l^k(x) \equiv \left[ (2l+1) \frac{(l-k)!}{(l+k)!} \right]^{\frac{1}{2}} \frac{1}{2^l l!} \frac{d^{l+k}}{dx^{l+k}} (x^2-1)^l, \tag{7}$$

$\{Q_l^k(x)\}$  can be calculated by using the following recursive formulas:

$$\begin{cases} Q_0^0 = 1, & Q_k^k = \left[ (2k+1) \prod_{k'=1}^k \frac{k+k'}{4k'} \right]^{\frac{1}{2}} \quad (k > 0), \\ Q_{k+1}^k = \sqrt{2k+3} x Q_k^k, \\ Q_l^k = \frac{1}{D_{k,l}} x Q_{l-1}^k - \frac{D_{k,l-1}}{D_{k,l}} Q_{l-2}^k \quad (l \geq k+2), \end{cases} \tag{7}'$$

where  $D_{k,l} \equiv \left[ \frac{l^2 - k^2}{4l^2 - 1} \right]^{\frac{1}{2}}$ .

Considering an associated Legendre function  $\{p_l^k(x)\}$ , we have

$$p_l^k(x) = (1-x^2)^{k/2} \cdot Q_l^k(x). \tag{8}$$

It means that  $\{p_l^k(x)\}$  and  $\{Q_l^k(x)\}$  are one-to-one correspondent. Supposing  $A = p_l^k(x) \cos k\lambda$  and  $B = p_{l'}^{k'}(x) \begin{cases} \cos k'\lambda \\ \sin k'\lambda \end{cases}$ , where  $x = \cos \theta$ , we deal with the following nonlinear operations of spherical harmonics:  $AB, J(A, B)$  and  $\nabla A \cdot \nabla B$ . Using Eq.(8) and product formulas of trigonometric functions, we have

$$\begin{cases} A \cdot B = \frac{1}{2} (1-x^2)^{k_1/2} T_1(x) \begin{cases} \cos k_1 \lambda \\ \sin k_1 \lambda \end{cases} \\ \quad + \frac{1}{2} (1-x^2)^{k_2/2} T_2(x) \begin{cases} \cos k_2 \lambda \\ -S_2 \cdot \sin k_2 \lambda \end{cases}, \\ J(A, B) = \frac{1}{2} (1-x^2)^{k_1/2} T_3(x) \begin{cases} \sin k_1 \lambda \\ -\cos k_1 \lambda \end{cases} \\ \quad + \frac{1}{2} (1-x^2)^{k_2/2} T_4(x) \begin{cases} -S_2 \cdot \sin k_2 \lambda \\ -\cos k_2 \lambda \end{cases}, \\ \nabla A \cdot \nabla B = \frac{1}{2} (1-x^2)^{k_1/2} T_5(x) \begin{cases} \cos k_1 \lambda \\ \sin k_1 \lambda \end{cases} \\ \quad + \frac{1}{2} (1-x^2)^{k_2/2} T_6(x) \begin{cases} \cos k_2 \lambda \\ -S_2 \cdot \sin k_2 \lambda \end{cases}, \end{cases} \tag{9}$$

where  $k_1 = k+k'$ ,  $k_2 = |k-k'|$ ,  $l_1 = l+l'$ ,  $S_2 = \text{sign}(k-k')$  and

$$\begin{cases} T_1(x) = Q_l^k \cdot Q_{l'}^{k'}, \\ T_2(x) = (1-x^2)^{\frac{k_1-k_2}{2}} Q_l^k \cdot Q_{l'}^{k'}, \\ T_3(x) = k' Q_{l'}^{k'} \frac{dQ_l^k}{dx} - k Q_l^k \frac{dQ_{l'}^{k'}}{dx}, \end{cases}$$

$$\begin{cases}
 T_1(x) = -2kk'x(1-x^2)^{\frac{k_1-k_2-2}{2}} Q_l^k \cdot Q_{l'}^{k'} \\
 \quad + (1-x^2)^{\frac{k_1-k_2}{2}} \left( k' Q_{l'}^{k'} \frac{dQ_l^k}{dx} + k Q_l^k \frac{dQ_{l'}^{k'}}{dx} \right), \\
 T_3(x) = -kk' Q_l^k Q_{l'}^{k'} + (1-x^2) \frac{dQ_l^k}{dx} \frac{dQ_{l'}^{k'}}{dx} \\
 \quad - x \left( k' Q_{l'}^{k'} \frac{dQ_l^k}{dx} + k Q_l^k \frac{dQ_{l'}^{k'}}{dx} \right), \\
 T_5(x) = kk'(1+x^2)(1-x^2)^{\frac{k_1-k_2-2}{2}} Q_l^k \cdot Q_{l'}^{k'} + (1-x^2)^{\frac{k_1+k_2+2}{2}} \frac{dQ_l^k}{dx} \frac{dQ_{l'}^{k'}}{dx} \\
 \quad - x(1-x^2)^{\frac{k_1-k_2}{2}} \left( k' Q_{l'}^{k'} \frac{dQ_l^k}{dx} + k Q_l^k \frac{dQ_{l'}^{k'}}{dx} \right)
 \end{cases} \quad (10)$$

It is easy to prove that  $T_1$ ,  $T_3$ ,  $T_5$  and  $T_2$ ,  $T_4$ ,  $T_6$  are all polynomials relative to  $x$ , and their degrees are not above  $l_1 - k_1$  and  $l_1 - k_2$ , respectively. Thus, taking  $\{Q_{l'}^{k_2} | l' = k_1, k_1+1, \dots\}$  and  $\{Q_{l'}^{k_1} | l' = k_2, k_2+1, \dots\}$  as the basis in the polynomial function space, respectively, we are able to expand  $T_1$ ,  $T_3$ ,  $T_5$  and  $T_2$ ,  $T_4$ ,  $T_6$  in the following forms:

$$\begin{cases}
 T_{2s-1} = \sum_{l'=k_1}^{l_1} d_{k_1, l'}^{(s)} Q_{l'}^{k_1}, \\
 T_{2s} = \sum_{l'=k_2}^{l_1} d_{k_2, l'}^{(s)} Q_{l'}^{k_2}.
 \end{cases} \quad (S=1, 2, 3,) \quad (11)$$

Using (8) repeatedly we can obtain the spherical harmonic expansions of (9) as follows

$$\begin{cases}
 A \cdot B = \frac{1}{2} \sum_{l'=k_1}^{l_1} d_{k_1, l'}^{(1)} p_{l'}^{k_1} \left\{ \begin{array}{l} \cos k_1 \lambda \\ \sin k_1 \lambda \end{array} \right\} \\
 \quad + \frac{1}{2} \sum_{l'=k_2}^{l_1} d_{k_2, l'}^{(1)} p_{l'}^{k_2} \left\{ \begin{array}{l} \cos k_2 \lambda \\ -S_2 \cdot \sin k_2 \lambda \end{array} \right\}, \\
 J(A, B) = \frac{1}{2} \sum_{l'=k_1}^{l_1} d_{k_1, l'}^{(2)} p_{l'}^{k_1} \left\{ \begin{array}{l} \sin k_1 \lambda \\ -\cos k_1 \lambda \end{array} \right\} \\
 \quad + \frac{1}{2} \sum_{l'=k_2}^{l_1} d_{k_2, l'}^{(2)} p_{l'}^{k_2} \left\{ \begin{array}{l} -S_2 \cdot \sin k_2 \lambda \\ -\cos k_2 \lambda \end{array} \right\}, \\
 \nabla A \cdot \nabla B = \frac{1}{2} \sum_{l'=k_1}^{l_1} d_{k_1, l'}^{(3)} p_{l'}^{k_1} \left\{ \begin{array}{l} \cos k_1 \lambda \\ \sin k_1 \lambda \end{array} \right\} \\
 \quad + \frac{1}{2} \sum_{l'=k_2}^{l_1} d_{k_2, l'}^{(3)} p_{l'}^{k_2} \left\{ \begin{array}{l} \cos k_2 \lambda \\ -S_2 \cdot \sin k_2 \lambda \end{array} \right\}.
 \end{cases} \quad (12)$$

The main operation concerned in formulas (9)–(12) is algebraic operation of polynomials, which can easily be performed by computer program (cf. [5]). In fact, we have written such a set of Fortran programs that all the operations concerned in solving Eqs. (5) and (6) are

able to be completed by computer.

IV. NONLINEAR HAURWITZ WAVES IN A TWO-LEVEL MODEL

By considering a two-level model (cf. Fig. 1), assuming Eqs. (5) and (6) to have a set of travelling-wave solutions propagating along  $\lambda$ -direction at a phase speed  $c=c_0+ec_1+\dots$  and taking Phillips' formula as the 0-Ax to the solution, Eqs. (5) and (6) can be recast into the following forms:

$$\left. \begin{aligned} \Psi_{0,k-\frac{1}{2}} &= -\hat{\Omega}_{k-\frac{1}{2}} \cos \theta + \hat{A}_{k-\frac{1}{2}} P_n^m(\cos \theta) \cos m\lambda, \\ c_{0,k-\frac{1}{2}} &= \hat{\Omega}_{k-\frac{1}{2}} \cdot \bar{\mu}^{-1} \left( 1 - \frac{2}{n(n+1)} \right) - \delta_\mu \cdot \bar{\mu} \cdot \frac{1}{n(n+1)}, \\ \hat{\Delta} \phi'_{0,k-\frac{1}{2}} &= \cos \theta \hat{\Delta} \Psi_{0,k-\frac{1}{2}} - \varepsilon N(\Psi_{0,k-\frac{1}{2}}), \\ T'_{0,k} &= -\frac{\sigma_k}{\varepsilon^* \Delta \sigma} (\phi'_{0,k+\frac{1}{2}} - \phi'_{0,k-\frac{1}{2}}), \\ p'_{0,0} &= \frac{\bar{P}_2}{RT_0} \phi'_{0,1/2}, \end{aligned} \right\} (k=1, 2, 3)$$

$$\left. \begin{aligned} T'_{0,k} &= -\frac{\sigma_k}{\varepsilon^* \Delta \sigma} (\phi'_{0,k+\frac{1}{2}} - \phi'_{0,k-\frac{1}{2}}), \\ p'_{0,0} &= \frac{\bar{P}_2}{RT_0} \phi'_{0,1/2}, \end{aligned} \right\} (k=1, 2)$$

and

$$\left. \begin{aligned} \phi'_{2, \frac{3}{2}} &= \delta''' \delta^* \left( \frac{\sigma}{S^2} \right)_{\frac{3}{2}} \left[ \frac{\partial}{\partial t} T'_{0, \frac{3}{2}} + \mathcal{J}(\Psi_{0, \frac{3}{2}}, T'_{0, \frac{3}{2}}) \right], \\ \hat{\Delta} X_{2,k} &= - \left[ \frac{3-2k}{\Delta \sigma} \phi'_{2, \frac{3}{2}} + \delta'' \left( -c_{0, \frac{3}{2}} \frac{\partial}{\partial \lambda} p'_{0,0} + \mathcal{J}(\Psi_{0,k}, p'_{0,0}) \right) \right], \\ \hat{\Omega}_k \bar{\mu}^{-1} - c_{0,k} \bar{\mu} (1 + \hat{\Delta}) \frac{\hat{\partial}}{\partial \lambda} \Psi_{1,k} &= c_{1,k} \bar{\mu} \frac{\hat{\partial}}{\partial \lambda} \hat{\Delta} \Psi'_{0,k} - \cos \theta \cdot \hat{\Delta} X_{1,k} \\ &\quad - \mathcal{J}(\Psi'_{0,k}, (1 + \hat{\Delta}) \Psi_{1,k}), \\ c_{1,k} &= \frac{1}{m \hat{A}_k} \left\{ \cos \theta \cdot \hat{\Delta} X_{2,k} \right\}_{m,n}, \\ \hat{\Delta} \phi'_{1,k} &= \cos \theta \cdot \hat{\Delta} \Psi_{1,k} - \varepsilon N_1(\Psi_{0,k}, \Psi_{1,k}), \\ T'_{1,k} &= -\frac{\sigma_k}{\varepsilon^* \Delta \sigma} (\phi'_{1,k+\frac{1}{2}} - \phi'_{1,k-\frac{1}{2}}), \quad (k=1, 2) \\ p'_{0,0} &= \frac{\bar{P}_2}{RT_0} \phi'_{0,1/2}, \end{aligned} \right\} (k=1, \frac{3}{2}, 2)$$

where the second subscripts of variables denote their level's numbers and  $\Psi'_0$  represents the non-zonal part of  $\Psi_0$ .

The fourth equation of (14) shows that the first-order correction (hereafter referred to as 1-Cr) of the phase speed,  $c_1$ , depends on either the divergence or the amplitude of the wave. It is just the character of nonlinear waves in compressible fluid. In fact,  $c_1$  also depends on the baroclinicity of the wave from the first two equations of (14).

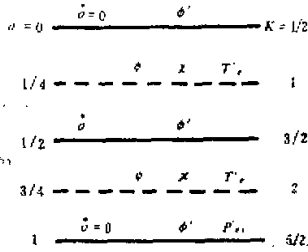


Fig. 1. Distributions of variables in the two-level model.

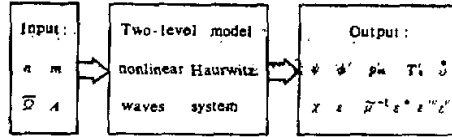


Fig. 2. Function of the two-level model nonlinear Haurwitz wave system.

In order to get the 1-Cr of the stream function,  $\Psi_{1,k}$ , the following iterative formulas

$$\begin{cases} (\hat{\Delta}_{k,\bar{\mu}}^{-1} - c_{0,k,\bar{\mu}})(1 + \hat{\Delta}) \frac{\partial \Psi_{1,k}^{(0)}}{\partial \lambda} = G_k, \\ (\hat{\Delta}_{k,\bar{\mu}}^{-1} - c_{0,k,\bar{\mu}})(1 + \hat{\Delta}) \frac{\partial \Psi_{1,k}^{(v+1)}}{\partial \lambda} = G_k - J[\Psi_{0,k}^{(v)}, (1 + \hat{\Delta})\Psi_{1,k}^{(v)}], \\ G_k \equiv c_{1,k,\bar{\mu}} \frac{\partial \hat{\Delta} \Psi_{0,k}^{(v)}}{\partial \lambda} - \cos \theta \hat{\Delta} X_{z,k}, \end{cases} \quad (15)$$

are used in solving the third equation of (14). The iteration does not stop until  $\|\Psi_{1,k}^{(v+1)} - \Psi_{1,k}^{(v)}\| < \frac{\epsilon}{2}$ , where  $v$  is the iterative index and  $\|\cdot\|$  represents the  $L_2$ -norm on the surface of unit sphere.

By using the algorithm described in Section III, the solving of Eqs. (13), (14) and (15) can be carried out automatically in computer. Thus, we can obtain a calculating system of nonlinear Haurwitz waves in the two-level model (cf. Fig. 2), which can be used to investigate nonlinear Haurwitz waves and to provide the initial conditions for testing of numerical models. One of important things is to select the parameters of the 0-Ax reasonably. With regard to Phillips' formula, taking  $L^* = a/\sqrt{n(n+1)}$ ,  $F^* = \|F\|^{(n+1)}$ , we have  $\epsilon \geq 0.3$ . It means that the corresponding Haurwitz wave may not be a better approximate solution to the primitive equations. Actually, several experiments<sup>[7-9]</sup> have revealed that the wave could not keep its shape unchanged during the time integration.

V. NUMERICAL EXPERIMENTS

Take a set of the model's parameters and the 0-Ax parameters as follows:

$$\begin{aligned} p_s &= 200 \text{ hPa}, \quad p_b = 1013 \text{ hPa}, \quad T_s = 288 \text{ K}, \quad \bar{c}_s = 120 \text{ m s}^{-1}; \\ m &= 4, \quad n = 5, \\ \bar{\Omega}_{k-\frac{1}{2}} &= (0.7331, 0.6879, 0.7029) \times 10^{-5} \text{ s}^{-1}, \\ A_{k-\frac{1}{2}} &= (0.5499, 0.4652, 0.4992) \times 10^{-5} \text{ s}^{-1}. \end{aligned} \quad (k=1, 2, 3).$$

By inputting them into the calculating system, all components of the nonlinear Haurwitz wave are calculated and outputted in the forms of both spherical harmonic expansions and

grid fields. Table 1 gives the dimensionless norms and the corresponding characteristic quantities of all the variables.

Table 1. The Norms and Characteristic Quantities of the 0-Ax (Top) and 1-Cr (Bottom)

$F$	$\phi'_{0,1/2}$	$\phi'_{0,3/2}$	$p'_{0,0}$	$\hat{\Delta}\Psi_{0,1}$	$\hat{\Delta}\Psi_{0,2}$	$T'_{0,1}$	$T'_{0,2}$
$\ F\ $	0.99	0.91	0.94	3.36	3.28	0.24	0.27
$F^*$	6980 $\text{m}^2 \text{s}^{-2}$	6500 $\text{m}^2 \text{s}^{-2}$	81.6 hPa	2.23 $10^{-5} \text{s}^{-1}$	2.12 $10^{-5} \text{s}^{-1}$	0.94 K	1.02 K

$F$	$\phi'_{1,1/2}$	$\phi'_{1,3/2}$	$p'_{1,2}$	$\hat{\Delta}\Psi_{1,1}$	$\hat{\Delta}\Psi_{1,2}$	$T'_{1,1}$	$T'_{1,2}$	$\hat{\Delta}\chi_{1,1}$	$\hat{\Delta}\chi_{1,2}$	$\hat{\sigma}_{1,3/2}$
$\ F\ $	0.19	0.08	0.03	0.20	0.08	0.31	0.36	0.26	0.13	0.04
$F^*$	190 $\text{m}^2 \text{s}^{-2}$	80 $\text{m}^2 \text{s}^{-2}$	0.4 hPa	0.18 $10^{-5} \text{s}^{-1}$	0.08 $10^{-5} \text{s}^{-1}$	0.19 K	0.22 K	0.29 $10^{-5} \text{s}^{-1}$	0.19 $10^{-5} \text{s}^{-1}$	0.04 $10^{-4} \text{s}^{-1}$

The corresponding dimensionless parameters are as follows:

$$\begin{aligned} \varepsilon \approx \bar{\mu}^{-1} \approx \varepsilon^* \approx 0.18, \\ \varepsilon'' \approx 2.0\varepsilon, \quad \varepsilon''' \approx 2.4\varepsilon. \end{aligned}$$

It shows that the solution given by our system satisfies the magnitude principle of perturbation analysis and meets the requirements posed in Section II.

Table 2. The Dimensionless Phase-Speed  $c_0$  and the Corresponding Correction  $c_1$

$k$	$c_0$	$c_1$
1	$0.665 \times 10^{-1}$	$-0.442 \times 10^{-1}$
2	$0.612 \times 10^{-1}$	$-0.152 \times 10^{-1}$

Table 2 gives the 0-Ax and the 1-Cr of the dimensionless phase-speed at both the two levels. Using them, we are able to calculate the theoretical phase-speed of the nonlinear wave

$$(c_0 + \varepsilon c_1)_k \times \frac{180}{\pi} \times \frac{86400}{24} \approx 7.7^\circ \text{day}^{-1} \quad (k=1,2).$$

Figs. 3—8 show the distributions of the 0-Ax and the 1-Cr of the geopotential height and the vorticity at level 1, the distribution of the divergence at level 1 and the distribution of the  $\sigma$ -vertical velocity at level 3/2.

In order to test properties of the baroclinic Haurwitz wave, we have performed two long-term integrations with the initial conditions given by 0-Ax and 1-Ax, respectively,



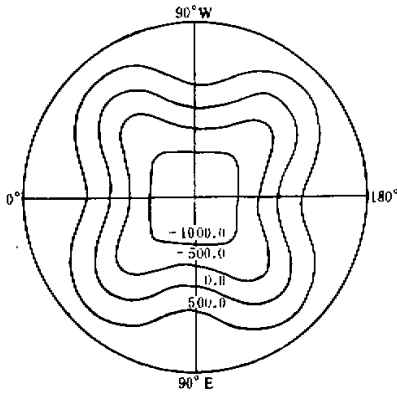


Fig. 3.  $\frac{1}{g} \phi'_{1,t}$  (unit: m).

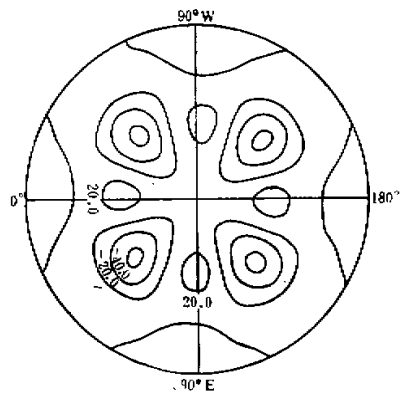


Fig. 4.  $\frac{\epsilon}{g} \phi'_{1,t}$  (unit: m).

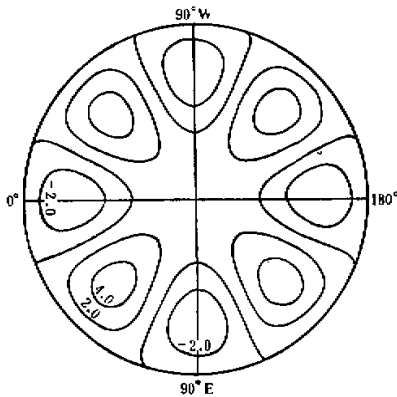


Fig. 5.  $\Delta\psi_{1,t}$  (unit:  $10^{-5} \text{s}^{-1}$ )

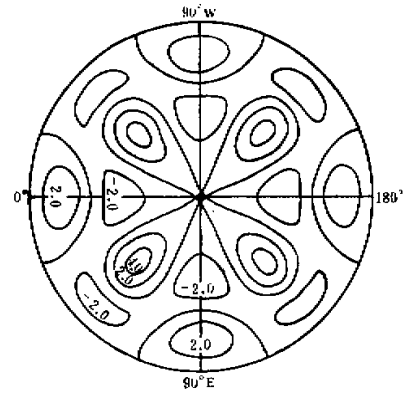


Fig. 6.  $\epsilon\Delta\psi_{1,t}$  (unit:  $10^{-5} \text{s}^{-1}$ )

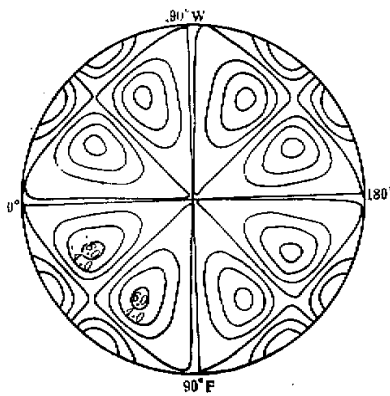


Fig. 7.  $\epsilon^2\Delta\chi_{2,t}$  (unit:  $10^{-7} \text{s}^{-1}$ )

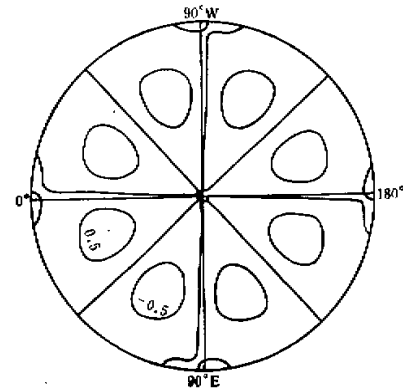


Fig. 8.  $\epsilon^2\sigma_{2,t}$  (unit:  $10^{-7} \text{s}^{-1}$ )

using the numerical global model developed by ourselves<sup>(10)</sup>.

The model is a two-level global primitive equation model in  $(\theta, \lambda, \sigma, t)$  coordinates. The vertical distribution of variables is the same as shown in Fig. 1 except  $v_\theta, v_\lambda$  being used instead of  $\Psi, \chi$ . Arakawa's C-grid is used in horizontal and the resolution is  $4^\circ \times 5^\circ$ . The finite-difference scheme of the model is designed to conserve the total mass and the total "available" energy<sup>(10)</sup> of the numerical solution. The leap-frog method with Robert's time filtering and the Fourier filtering in Polar regions is used in time integration.

Fig. 9 shows the 50th day distribution of the geopotential height at level 1 under the corresponding initial conditions (dashed line). By that time, the wave had already moved through 369 degrees longitude from west to east. The calculated phase-speed averaged over the fifty days is about  $7.38^\circ$  per day and just  $0.32^\circ$  per day slower than the theoretical value. In several experiments<sup>[7-9, 11, 12]</sup>, the phase-speed errors are above  $1^\circ$  per day. It

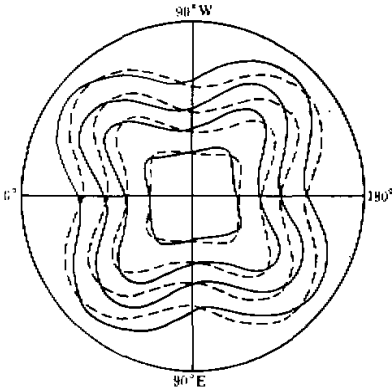


Fig. 9. The 50th day distribution (solid lines) of the geopotential height of 1-Ax under initial conditions (dashed lines).

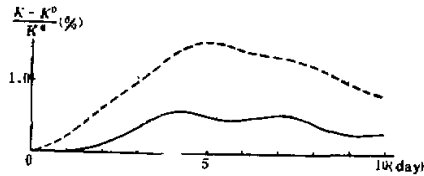


Fig. 10. The variation of the kinetic energy. Dashed line—linear wave; Solid line—nonlinear wave.

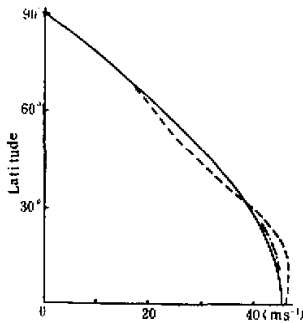


Fig. 11. The profile of the zonal wind averaged over the first ten days. Dashed line—linear wave; Solid line—initial condition; Dotted-dashed line—nonlinear wave.

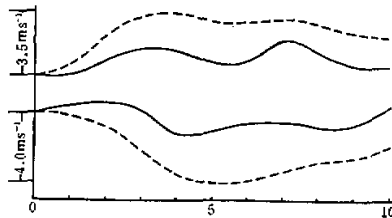


Fig. 12. The variation of the zonal wind at  $20^\circ\text{N}$  (above) and  $50^\circ\text{N}$  (below). Dash lines—linear waves; Solid lines—nonlinear waves.

should be pointed out that one of the sources of errors may be the use of the inexact reference phase-speed  $c_0$ . It can also be seen that the shape of the wave is still perfect after a long-term integration. A further calculation shows that the average deformation error of the geopotential height by the 50th day is about  $100 \text{ m}^2 \text{ s}^{-2}$ .

The behaviour of the geopotential height at level 2 and the surface pressure are very similar to the above-mentioned. However, the disturbance temperature, which is a secondary quantity in a weak baroclinic process, displays an obvious periodic oscillation.

Figs. 10 and 11 give a comparison between the linear and nonlinear Haurwitz waves, which shows that the nonlinear wave is more accurate than the linear one.

Fig. 12 gives the variation of the zonal wind at two special latitudes. It shows that the nonlinear interaction between the wave and the zonal flow in the evolution process of the linear wave is stronger than the nonlinear wave.

#### REFERENCES

- [ 1 ] Haurwitz, B., *J. Marine Research*, III(1940), 254—267.
- [ 2 ] Phillips, N. A., *Mon. Wea. Rev.*, 87(1959), 335—345.
- [ 3 ] 曾庆存, 数值天气预报的数学物理基础, 第一卷, 科学出版社, 北京, 1979.
- [ 4 ] 张学洪, 包宁, 曾庆存, 地球物理流体力学会议论文汇编, 舟山, 1984.
- [ 5 ] Zhang Xuehong., *Adv. Atmos. Sci.*, 2(1985), 2:167—177.
- [ 6 ] Fjørtoft, R., *Tellus*, 5(1953), 225—230.
- [ 7 ] Hoskins, B. J., *Quart. J. Roy. Meteor. Soc.*, 99(1973), 723—745.
- [ 8 ] Umschied, L. and P. R. Bannan, *Mon. Wea. Rev.*, 105(1977), 618—635.
- [ 9 ] Nakamura, H., *J. Meteor. Soc. Japan*, 56(1978), 175—186.
- [ 10 ] 曾庆存, 张学洪, 包宁, 袁重光, 地球物理流体力学论文汇编, 舟山, 1984.
- [ 11 ] Bourke, W., *Mon. Wea. Rev.*, 100(1972), 683—689.
- [ 12 ] Merilees, P. E., *Atmosphere*, 12(1974), 77—96.